	NOT Scientific Report **5 m/s ten-month stability with FIES**	**Date: February 11, 2025** **Author: Jeppe Sinkbaek Thomsen** **jet@phys.au.dk** **Version: 1** **Page 1 of 16**

Author(s)	Function	Date and Signature
Jeppe Sinkbaek Thomsen University of Bologna, Aarhus University	Main author, FIES user	
John Telting Nordic Optical Telescope	FIES instrument astronomer	
Joonas Viuho Nordic Optical Telescope, University of Copenhagen	Instrument scientist	
Approved by:		
Authorized by		

CHANGE RECORD

ISSUE	DATE	SECTION/PAGE AFFECTED	REASON/INITIATION DOCUMENTS/REMARKS
Draft	11/12/2024	All	Document initiated, Author: Jeppe
Draft	15/12/2024	All	Proof-read, Author: Jeppe
Draft	06/01/2025	All	Feedback from John and Joonas, Author: Jeppe
Final v. 1	11/02/2025	All	Instrument layout, hardware considerations. Author: Joonas, Jeppe

TABLE OF CONTENTS

1. PREFACE......4

1.1 REFERENCE DOCUMENTS 4
1.2 ABBREVIATIONS AND ACRONYMS......4

2. INTRODUCTION AND CURRENT INSTRUMENT OVERVIEW......4

3. SUMMARY ON FIES SHORT-TERM RV STABILITY......4

4. OBSERVATIONS FOR LONG-TERM CHARACTERIZATION......6

5. SPECTRAL EXTRACTION WITH FIESTOOL......6

6. THAR DRIFT......7

7. RADIAL VELOCITY MEASUREMENT FROM SIG DRA OBSERVATIONS......9

8. BARYCENTRIC CORRECTIONS......10

9. ORDER SYSTEMATICS FOR SIG DRA, AND INTERNAL RV UNCERTAINTY......11

10. STANDARD STAR RESULTS, WAVELENGTH REFIT EVERY NIGHT......12

11. STANDARD STAR RESULTS, CONSTANT WAVELENGTH SOLUTION......12

12. UNEXPLORED (POTENTIAL) SYSTEMATIC SOURCES OF UNCERTAINTY......14

13. ACTION POINTS, SOFTWARE......14

14. ACTION POINTS, HARDWARE......15

15. FINAL WORDS......15

Date: February 11, 2025
Author: Jeppe Sinkbaek Thomsen
jet@phys.au.dk
Version: 1

1. Preface

1.1 Reference Documents

Reference	Author	Date	Title
RD 01	J.H. Telting et al.	2014	FIES: The high-resolution Fiber-fed Echelle Spectrograph at the Nordic Optical Telescope
RD 02	J. S. Thomsen	13/04/2023	FIES velocity stability
RD 03	P. Butler et al.	2017	The LCES HIRES/Keck precision Radial Velocity exoplanet survey
RD 04	Redman et al.	2014	The Spectrum of Thorium from 250 nm to 5500 nm: Ritz Wavelengths and Optimized Energy Levels
RD 05	Rucinski	1999	Determination of Broadening Functions Using the Singular-Value Decomposition (SVD) Technique
RD 06	Coelho et al.	2005	A library of high resolution synthetic stellar spectra from 300 nm to 1.8 micro-meter with solar and alpha-enhanced composition
RD 07	Wright & Eastman	2014	Barycentric corrections at 1 cm s^-1 for precise Doppler Velocities

1.2 Abbreviations and Acronyms

RV	Radial Velocity
sig Dra	Sigma Draconis (star)
ThAr	Thorium Argon emission lamp
BC	Barycentric correction
STD	Standard deviation
SNR	Signal-to-Noise Ratio
OB	Observing block
DOF	Degrees of freedom

2. Introduction and current instrument overview

This report details the findings of a ~10 month observing run to monitor the long-term stability of the Fibre-fed Echelle Spectrograph (FIES) using standard star observations of sig Dra. The Nordic Optical Telescope provided the observing time as technical time. I, Jeppe Sinkbaek Thomsen, came to la Palma for three weeks, Nov 20 – Dec 12 2024, to perform the data reduction and evaluation in collaboration with the instrument astronomer, John Telting, and instrument scientist Joonas Viuho. The trip was financially sponsored by the Instrument center for Danish Astronomy (IDA).

FIES is a fiber-fed white pupil échelle spectrograph originally designed for stellar spectroscopy **(RD 01)**. The original science case did not require as extreme environmental stability as is needed for cutting edge exoplanet research. Nevertheless, improvements on the long term RV stability have been made in the course of the years. Probably most importantly, the original round fibers were replaced with octagonal fibers providing better image scrambling. In 2019, the FIES grating was installed in a separate tank filled with Neon by the DTU exoplanet group lead by Lars Buchhave, providing both better mechanical stability and reducing turbulence-driven refractive index changes in proximity of the grating. The grating tank installation was followed up by an extensive testing and observing campaign with an etalon wavelength calibration source. As a part of this work with René Tronsgaard Rasmussen and Graham Cox, the fan and heater placement and control was optimized leading to the current state of the FIES building thermal control. In the end, the etalon itself showed short term (<1min) drifts that were not possible to correct for, leaving one to search for

Date: February 11, 2025
Author: Jeppe Sinkbaek Thomsen
jet@phys.au.dk
Version: 1

alternative calibration strategies. The FIES exposure meter was suspected to cause instrumental drift. This was later investigated and confirmed during my NOT studentship, where the exposure meter was found to heat the pedestal of the intermediate focus folding mirror, tilting it due to differential thermal expansion **(RD 02)**. The exposure meter has now been moved outside the inner enclosure.

FIES is installed in its own building outside the telescope to ensure mechanical stability. Air temperatures inside the building, and within the FIES inner and outer enclosures are controlled. The FIES building is kept at elevated temperature such that it is warmer than the outside ambient night time air temperature throughout the year. The air volumes inside the enclosure are kept at slightly elevated temperature respective to the building temperature. The FIES building front room is sealed less well than the spectrograph room itself, and it exchanges air with the outside. The front room temperature is kept at +19°C but undergoes oscillation of ±1°C. The spectrograph room is stabilized to +20°C with the heater and fan layout optimizing the temperature stability of the air volume, see Fig 1. The outer (white box) enclosure is stabilized at +21°C, again circulated by fans. Two of the white box heaters are placed on the aluminum frame of the inner enclosure (black box) and the heater air is circulated with fans. The air inside the black box is not heated, but it is still circulated by two fans, see Fig 2. The Fig 2 also indicates the naming and current location of available temperature sensors. The optical table is thermally isolated from the ground. To give an idea of the dimensions in the figure, FIES collimator focal length ~1.5m and the optical bench is 3m x 1.25m.

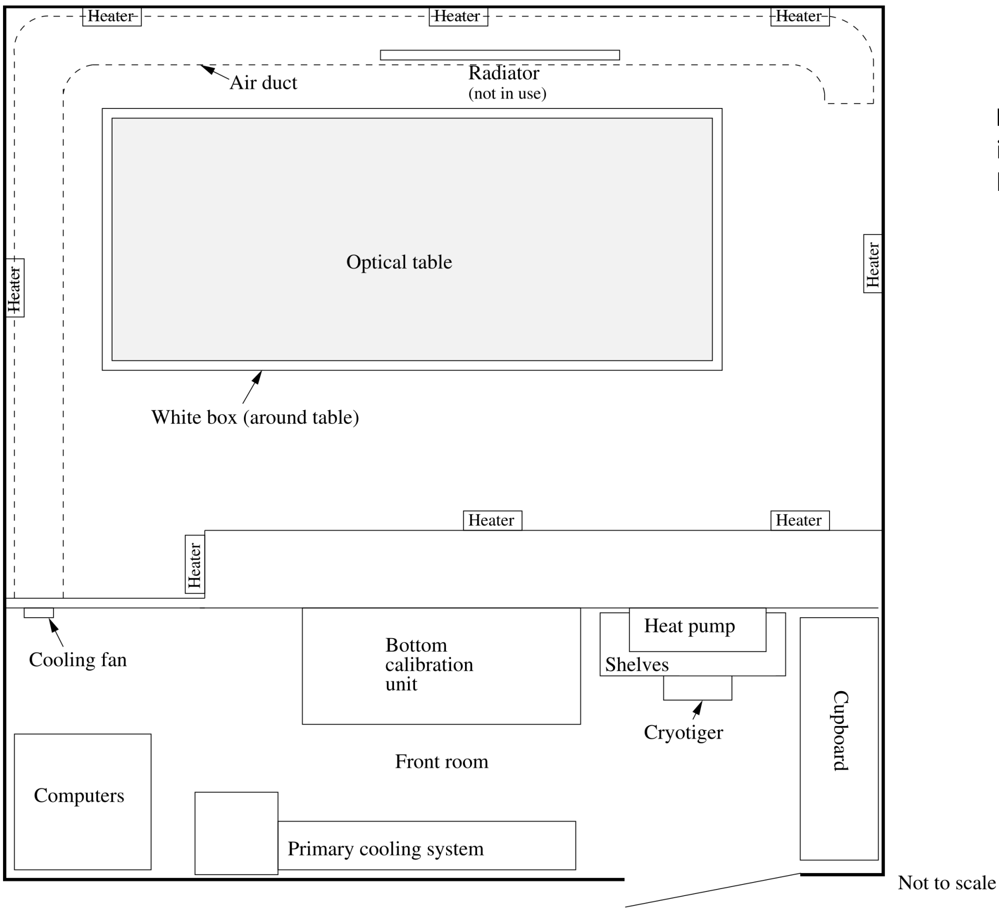

Figure 1. Top-down illustration of the FIES building.

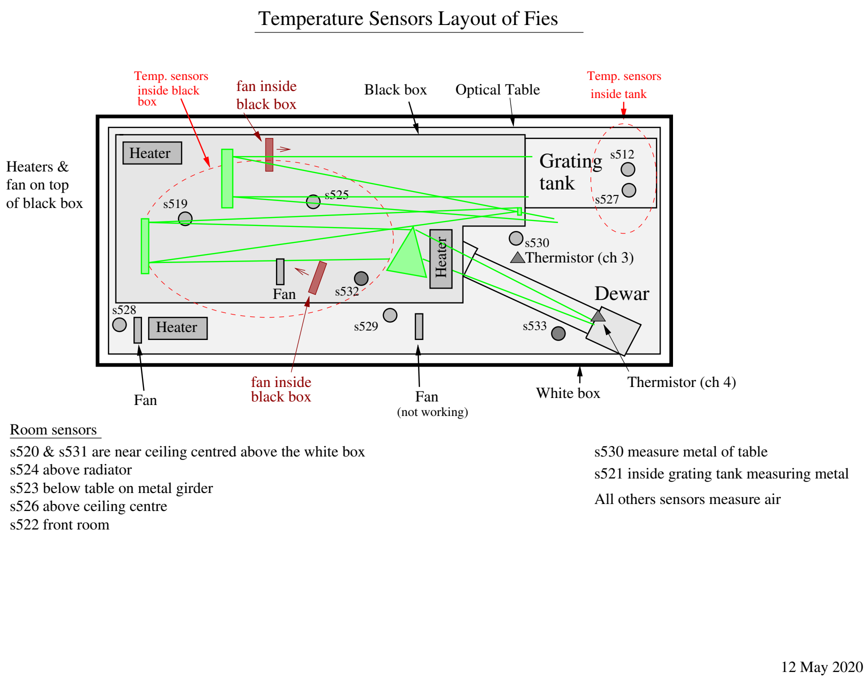

Figure 2. Temperature sensor and optical layout of the optical table (see Fig. 1).

3. Summary on FIES short-term RV stability

For context, I first summarize the short-term stability of the instrument. During my 10 month studentship at NOT in 2022-2023, I tested the RV stability of FIES over individual nights using the drift of emission lines of ThAr spectra as an analogue to the RV measured from stellar absorption lines **(RD 02)**. The result was that, for a single night with a fixed wavelength solution, under ideal weather and instrument conditions the high-precision RV operating mode of FIES could achieve a STD of ~1 m/s for exposures below an hour, using the sandwich correction illustrated in Fig. 3 and Fig. 4. For the worst nights, 15-30 minute stellar exposures could be corrected down to approximately 1.5-2.0 m/s.

Another major result of the studentship project was that the FIES exposure meter was thoroughly documented to cause a significant instrument drift (up to ~100 m/s) when powered on and off, due to proximity heating of the front part of the (very long) mounting bracket for the flat folding mirror close to secondary focus, which caused the mirror to tilt due to thermal expansion of one end of the mount. The exposure meter was subsequently moved on top of, outside, the spectrograph box, and a pick-off mirror guides light from the bottom of the dispersed beam to it.

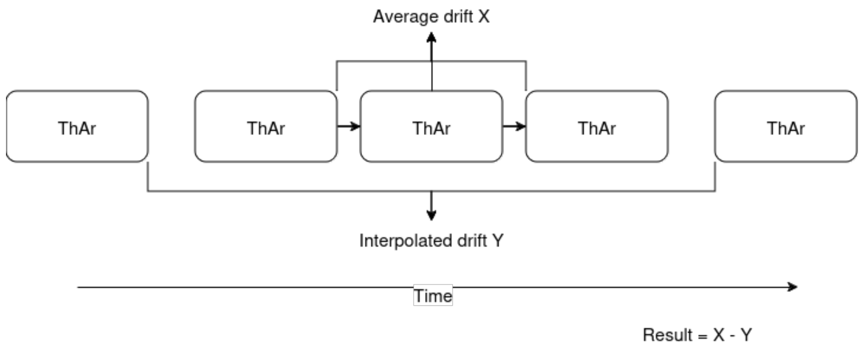

Figure 3. Illustration of the "simulated sandwich-mode" observation where a long exposure is simulated by averaging the drift of several shorter ThAr exposures. Thereafter, the nearest neighboring ThAr spectra are used to interpolate a correction, mimicking a typical high-precision RV stellar observing procedure with FIES.

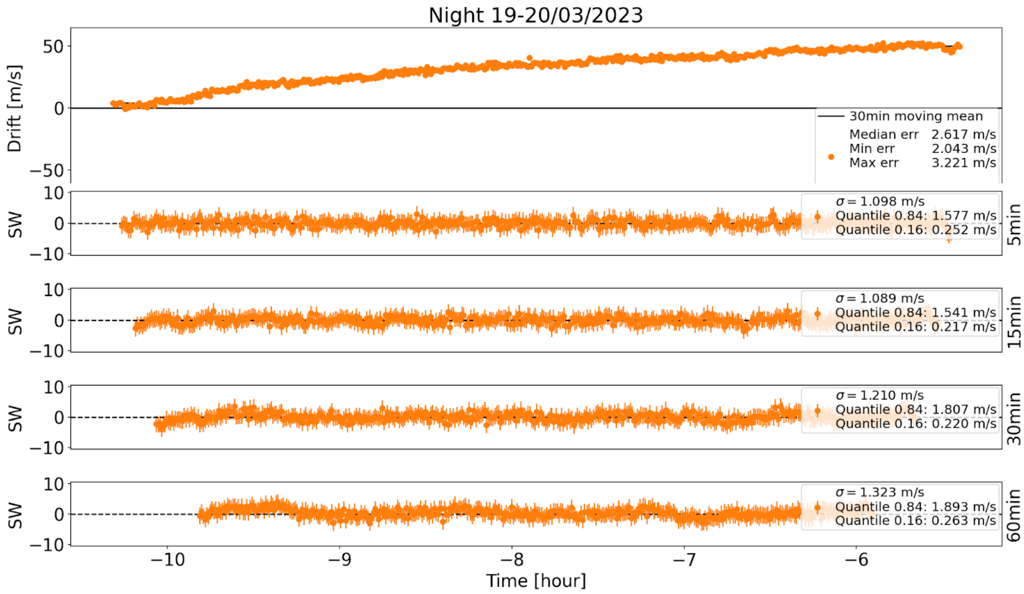

Figure 4. ThAr drifts measured for an ideal night, and the residual from the sandwich mode correction illustrated in Fig. 3 for different simulated exposure times. SW="Sandwich corrected".

The studentship observations with the ThAr lamps were performed specifically to test the short-term precision of the spectrograph in conditions where all the exposures could share the same calibration. The spectrograph reduction is typically re-calibrated between every night to remove long-term variations, the effect of which was not investigated in detail in the studentship project. For some nights, the data came from the top ThAr unit (through the science fiber) while the telescope was parked at zenith, while for others, the calibration ThAr unit in the FIES building was used since it had higher throughput and observing cadence could therefore be increased. Therefore, changes in the light path through the fiber due to location on the sky and extension/unrolling of the science fiber was not investigated. The octagonal fibers, while producing a much more efficient scrambling of the incoming light than the previous circular fibers, will still not produce a perfectly scrambled image. To test the ability to calibrate for this, a normal observation run must be mimicked as closely as possible, including changes in orientation of the telescope over many different nights of the year.

4. Observations for long-term characterization

In order to characterize the long-term accuracy of the whole optical train of FIES (telescope and top calibration unit, fiber, spectrograph), we observed the RV standard star sig Dra for 10 months, with an approximate cadence of 7 days between each observation. This star is known to vary with an amplitude of only 1.4 m/s over a period of 2644 days **(RD 03)**. As a cool, slowly-rotating K0 dwarf, it has a wealth of narrow absorption lines making it ideal for RV study. Its location on the sky also means that it is observable from La Palma all night, most nights of the year at roughly similar airmass. Its brightness (V=4.7) allows for nominal SNR of 384 for 3x90s exposures at seeing 1.0" with the FIES high-resolution fiber (fiber 4). Since the observations were not optimized for highest altitude (they were always observed in direct succession to another specific observing block), we made use of the atmospheric dispersion corrector (ADC).

We chose a nightly observing mode illustrated by Fig. 5, where three consecutive exposures of 90 seconds are sandwiched between two ThAr exposures. Here we used the long (x4) exposure ThAr mode offered by the observatory OB system.

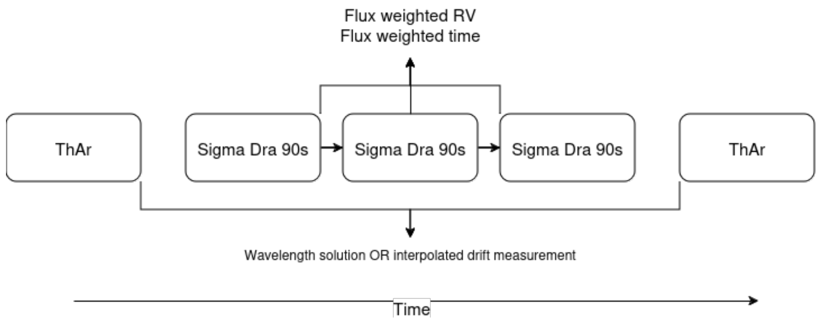

Figure 5. The observing structure of the sig Dra OB for each observation night. Here, the RV could be measured independently for each exposure, and a weighted average RV and mid-point of observation could then be produced, without relying on the exposure meter. The ThAr spectra could either be averaged and used to re-fit the wavelength solution every night, or be used to measure and interpolate an instrument drift.

Most nights, the ThAr lamp was switched on (and kept on) at least 20 minutes before the first ThAr was started, in order to let the lamp warm up to its equilibrium temperature. During my studentship, we found indications that the heating up of the ThAr might impact the perceived instrument drift by 5-10 m/s and take around 10min to stabilize. However, this was not confirmed with certainty. Therefore, to ensure homogeneity between the emission spectra of different nights as possible within the normal operating constraints of the telescope, we scheduled the ThAr lamp to be turned on at least 20min before observations of sig Dra. The two nights where the lamp might not have been warmed up before, April 21 and May 26, do not show statistically significant deviation in RV in the later analysis.

5. Spectral extraction with FIEStool

To either perform the wavelength calibration using time-averaged ThAr frames, or use one wavelength calibration for all nights, it was necessary to re-run the data reduction of all nightly calibration frames. For this purpose, the FIEStool virtual machine was downloaded, and FIEStool version 1.5.2 was installed on it.

Then, an automated script was set up to perform the reduction with *FIESscript.py*. An example without real data, along with instructions, configuration files and master frames, can be found at https://github.com/jsinkbaek/FIEStoolReduction. Master frames were provided by John Telting, taken from a nightly reduction from the main observatory pipeline.

During my three weeks on la Palma, John Telting produced an updated master linelist with 2200 lines from the IRAF ThAr linelist, and we verified that this improved nightly stability, when re-fitting the solution, by a few m/s over the use of the standard linelist with ~700 lines. The linelist on the previous link is the updated one with 2200 lines.
The IRAF linelist has old laboratory wavelengths, some of which have since been improved observationally, see f.ex. **RD 04**. Lines from **RD 04** are available in atmosphere wavelengths at https://www.nist.gov/pml/spectrum-th-ar-hollow-cathode-lamps. In the three weeks I was here, we did not find the time to test if a linelist with new laboratory wavelengths would improve over the IRAF linelist.

The final output spectra used for RV (and ThAr) analysis were the "_wave.fits" data files from FIEStool. Here, a wavelength solution has been applied but the orders have not been merged yet.

To estimate the self-reported ThAr drift of the FIEStool solution (from only the 2200 lines fitted by the pipeline), the IRAF package "ecreidentify" wavelength solution output files (called *ecwaveref* in the local FIEStool implementation), generated each time the wavelength solution is refitted, can be used.
They report, for each recovered emission line, the spectral and aperture order, the observed pixel, the observed wavelength from the polynomial fit, and the reference wavelength of the line.
As the last lines in the file, the coefficients of the 2D wavelength polynomial are reported.

For FIEStool, the 2D polynomial is a series of Chebyshev polynomials. For 2200 lines, John Telting fitted up to degree 4 (0-4) in both order and pixel space. The number of fitting coefficients C_mn then becomes 25 (5x5). The observed wavelength is described as a function of normalized pixel *x* and normalized order *o* in the following way:

$$\lambda(x,\ o)\ =\ \sum_{n=0}^{4}\sum_{m=0}^{4} C_{mn}P_m(x)P_n(o)$$

The normalization is

$$x\ =\ 2\left(x^* - (x_{max}+x_{min})/2\right)/(x_{max}-x_{min})$$
$$o\ =\ 2\left(o^* - (o_{max}+o_{min})/2\right)/(o_{max}-o_{min})$$

where xmax,min and omax,omin are reported in ecwaveref just before the fitting coefficients (but are typically 2062, 1, 154, and 64, respectively). The order o* here refers to the spectral order, not the aperture order.

6. ThAr drift

ThAr drift was estimated using two methods. In the first, the wavelength solution self-reported drift is measured using the exact 2200 lines employed in the wavelength fit re-performed each night. The wavelength residual is measured relative to the mean of each line, converted to m/s, and then all lines are averaged for a single night/spectrum. This is a lower limit estimate of the precision we have recovered by re-fitting the solution every night. The result can be seen in Fig. 6. We obtain a STD of 1.8 m/s this way.

$$LineDrift\ (i,x,o) = c\cdot\frac{\lambda - \langle\lambda\rangle_i}{\langle\lambda\rangle_i}$$

$$Drift_i\ =\ \langle LineDrift\rangle_{x,o}$$

$$\sigma_i = \sqrt{\frac{Var(LineDrift)_{x,o}}{nLines}}$$

$$i\ =\ night$$
$$c = speed\ of\ light$$

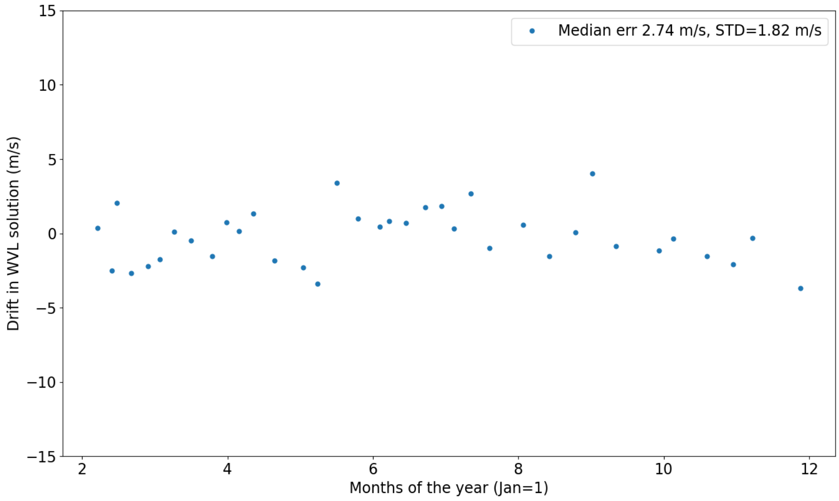

Figure 6. The average drift of the 2200 ThAr lines, after using them to fit the wavelength solution.

The other option is to use a code that measures a drift from all the pixels of the ThAr spectra, after the 2200 lines have been used to fit the wavelength solution. This will include both emission lines that are in, and not in, the polynomial fit. As such, it should be a more accurate estimate of the true variation. To perform this, I used the same method employed for my 10-month studentship project on the short-term stability: Empirical high-SNR template generation for each order from all the spectra, followed by least-squares fitting of the template to each order. This is the same method used to produce Fig. 4, taken from the studentship project. The result for the ThAr spectra of the new standard star OBs are shown in Fig. 7. Here, we obtain a STD of 6.8 m/s, which is 5 m/s higher than when only using the lines used for the wavelength solution fit. Such a significant difference can be caused either if a lot of the lines outside the 2200 change dramatically with time, or if the wavelength solution is significantly less accurate when moving away from the location of those 2200 reference lines. It is likely dominated by the latter uncertainty source, but we can verify that by comparing with the standard star observations themselves.

Figure 7. ThAr drift measured from all the pixel data of several orders. The drift measurement method is the same as for Fig. 4. However, for these ThAr spectra the wavelength solution has been re-fitted on each exposure independently.

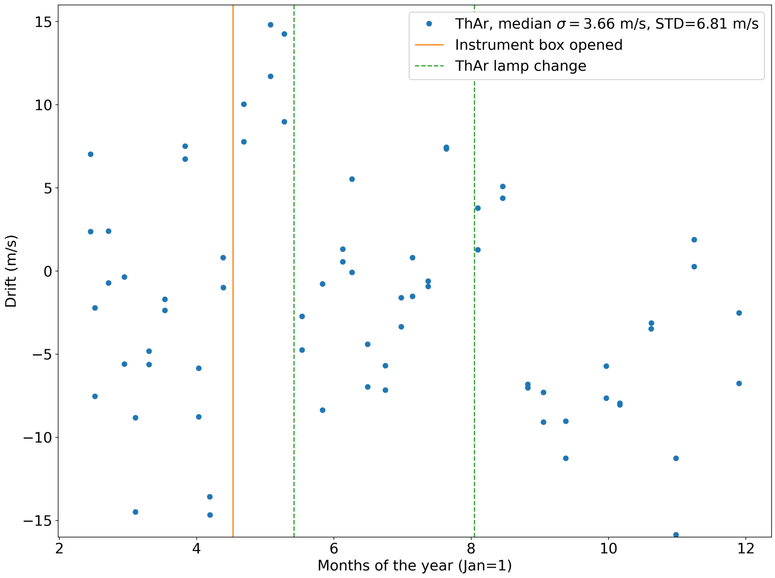

7. Radial velocity measurement from sig Dra observations

To measure RVs from sig Dra, I normalized the continuum of each spectral order to 1.0. There are many ways to do this, and it does not have to be absolutely perfect to produce good RVs (see right edge of Fig. 8, where it is poorly normalized).

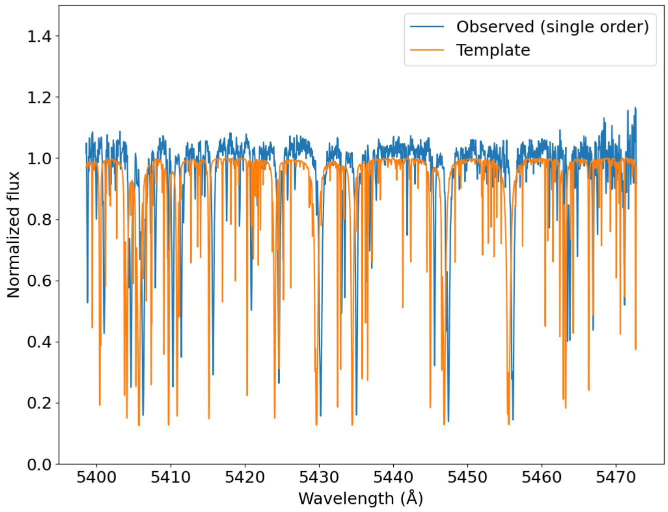

Figure 8. Observed spectrum (blue) and high resolution synthetic spectral template (orange), for a single spectral order.

Then, I resample the spectrum to 1.0 km/s wavelength spacing by interpolating and reduce the dimensionality of the data using the broadening function method **(RD 05)**. The broadening function method is conceptually similar to the cross-correlation formalism, but mathematically very different. A narrow-line template is required, which gets decomposed into principal components using singular value decomposition (SVD). Then, the decomposed template is used to solve for the line broadening function that the spectral template has to be convolved with to produce the observed spectrum. Conveniently, this line broadening function is a measurement of the average line profile of the star relative to the template. For this analysis, I used a template from **RD 06** with effective temperature of 5250K, logg=4.5, [Fe/H]=0.0 and [alpha/Fe]=0.0. I use 400 principal components for the template SVD which, with a wavelength step of 1 km/s, translates to an output broadening function interval of [-200, 200] km/s.

Then, I smooth the broadening function with a Gaussian filter with sigma=2 km/s to reduce linear noise obtained from using too many principal components and a narrow wavelength range. Finally, I fit a Gaussian line profile to the broadening function with least-squares to measure the radial velocity and estimate a formal error. This is illustrated in Fig. 9. I perform this reduction independently for aperture orders 17 to 66 (first order named 0), which corresponds to 4140-6530Å, for every single night. I also cut out away the first 30, and the last 50, pixels of each order since the noise becomes significantly higher (and the high wavelength side of the orders have an imperfect blaze correction / normalization). The formal error is used when producing an error-weighted mean RV in Sect. 8-10.

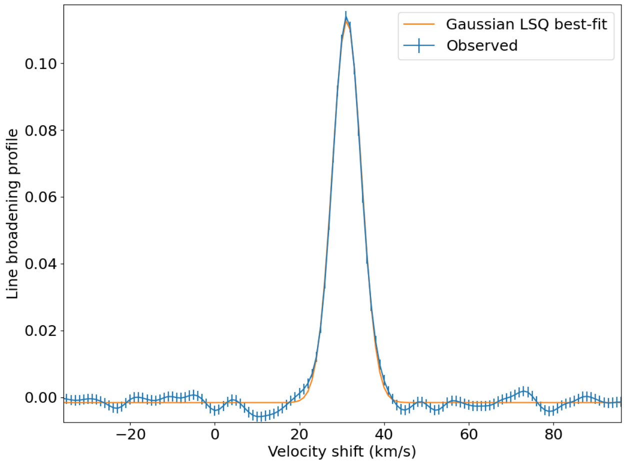

Figure 9. Average line broadening profile of the star for one order, measured using the broadening function method.

8. Barycentric corrections

As documented in **RD 07**, for high-precision radial velocity work the correction to account for the line-of-sight motion of the Earth around the solar barycenter cannot be accounted for in just an additive way (calculate BC, measure RV, RVtrue=RV+BC). The observed RV has to enter into the calculation of the correction, because a multiplicative cross-term is present in the calculation:

$$(1 + z_{\mathrm{meas}})(1 + z_B) - 1 = z_{\mathrm{true}}.$$

For our sig Dra observations, this is not the dominant noise-source, the difference between the two only reach peak-to-peak variation of <1 m/s (see Fig. 10), since the star is close to the celestial north pole.

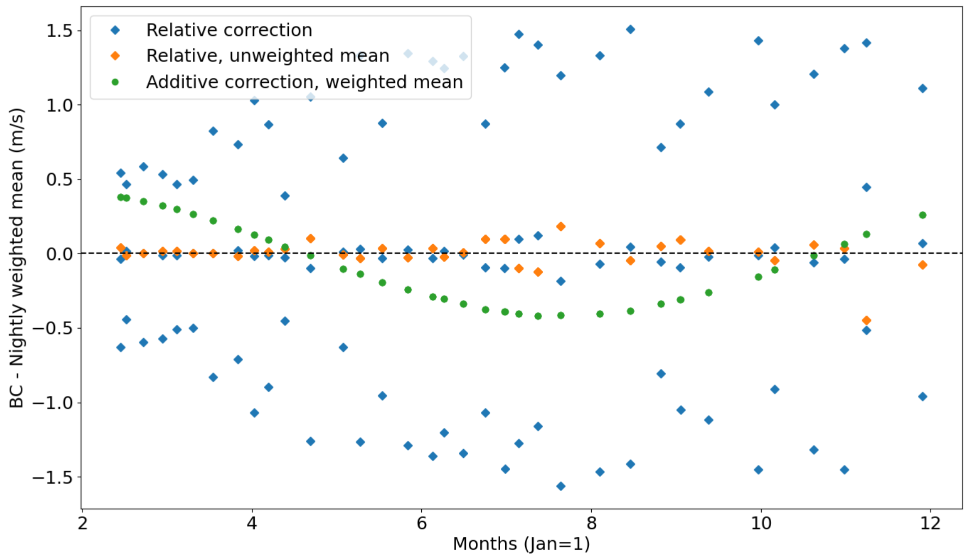

Figure 10. Difference in BC relative to weighted mean of night. Blue = individual spectra. Orange = unweighted mean. Green = BC where observed RV of star has not been included in the calculation.

To calculate barycentric corrections, I used the python package *barycorrpy* published with **RD 07** (https://zenodo.org/records/5148819). The overall practice outlined under "1 cm/s precision" in https://github.com/shbhuk/barycorrpy/wiki/02.-Getting-Started is followed where it is deemed feasible; the RV is measured first for each spectrum in order to perform the relative BC; the mid-point of observation time is taken as the weighted mid-point evaluated from the RV error of each exposure (although at this observation length and RV precision it is not a dominant error source, see Fig. 10); observatory position is taken as Long=17°53'06.3", Lat=+28°45'26.2", Alt=2382m (https://www.not.iac.es/telescope/tti/technical-details.html); and the stellar position and proper motion is taken from Gaia DR3 with epoch JD = 2457389 (J2016.0) (for this bright and well-studied system, the SIMBAD solution proved equally good).

9. Order systematics for sig Dra, and internal RV uncertainty

When fitting RVs on the sig Dra spectra with the wavelength re-calibrated every night, significant order-to-order systematics are observed on the order of +-0.8 km/s (see Fig. 11). However, it appears very stable across all the nights, and when correcting for the average, the nights start to look almost normally distributed (Fig. 12).

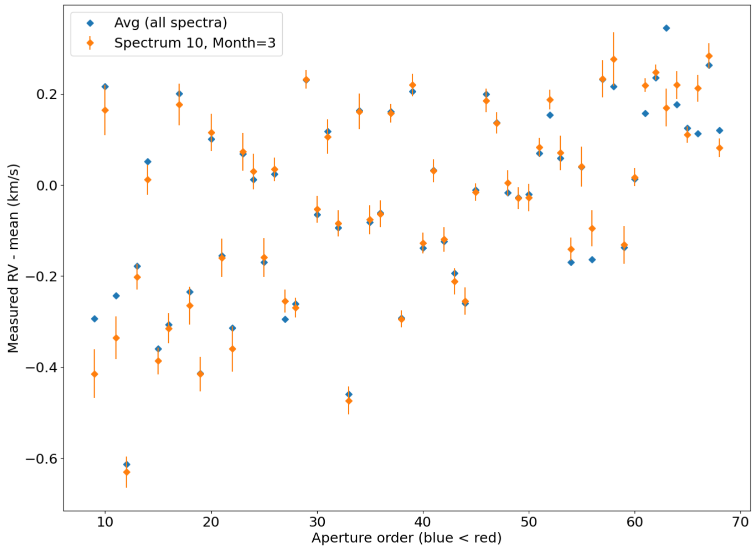

Fig 11. Measured RV variation vs aperture order. Showing a spectrum from a single night (orange) and the average of all nights.

After correcting the mean RV offset for each order (Fig. 9), the scatter in Fig. 10 is used to calculate an internal standard error for every single night, as STD/sqrt(Norders).

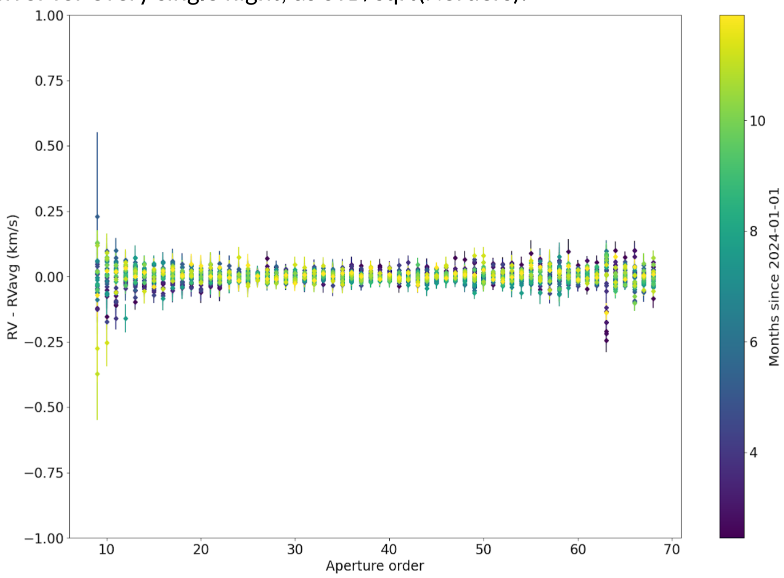

Figure 12. Fig. 11 for all spectra, after removing the average systematic.

10. Standard star results, wavelength refit every night

The nightly average RV measurements of sig Dra, corrected for motion along the solar barycenter, is shown in Fig. 13.

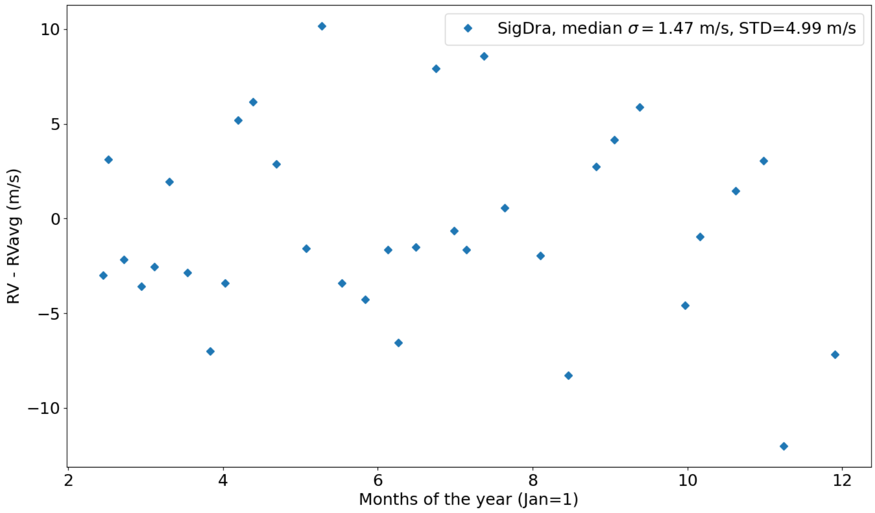

Figure 13. RV measurements of sig Dra, when re-fitting the wavelength solution every night.

The internal uncertainty calculated in Sect. 8 has a median of 1.5 m/s for all the nights. The mean RVs have a STD of 5 m/s over the 10 months of observing time. This is, to my knowledge, the best long term precision for FIES firmly reported for that long a time-span. This was obtained using the traditional reduction software FIEStool, but not using the data products of the observatory pipeline.

Using the ~700 ThAr lines typically employed by the automated FIEStool reduction, the STD was instead ~6.5 m/s. Wavelength solution stability is clearly a dominant source of uncertainty with the lower number of lines, and likely still is even when tripling the number of ThAr lines used.

Our best result with 5 m/s precision using 2200 ThAr lines for wavelength calibration is still not at the level of 1.8 m/s self-reported by the FIEStool wavelength fit. Since both the ThAr drift measurement of Fig. 7 and sig Dra show significantly higher scatter than IRAF reports for the wavelength solution, this indicates that the current limiting factor (when re-fitting every night) is the accuracy and precision of the wavelength fit in locations of the spectrum not close to the 2200 emission lines used.
To improve on that, the re-fitting procedure must be made more robust.

11. Standard star results, constant wavelength solution

The 1-2 m/s precision from a single night obtained during my studentship was achieved by giving all the spectra the same wavelength solution, and correcting for drifts measured using the neighboring ThAr spectra. I therefore found it relevant to investigate if this could be a suitable course of action over longer observing periods. In Fig. 14, plots similar to Fig. 12 and Fig. 13 are shown for the case where this is done.

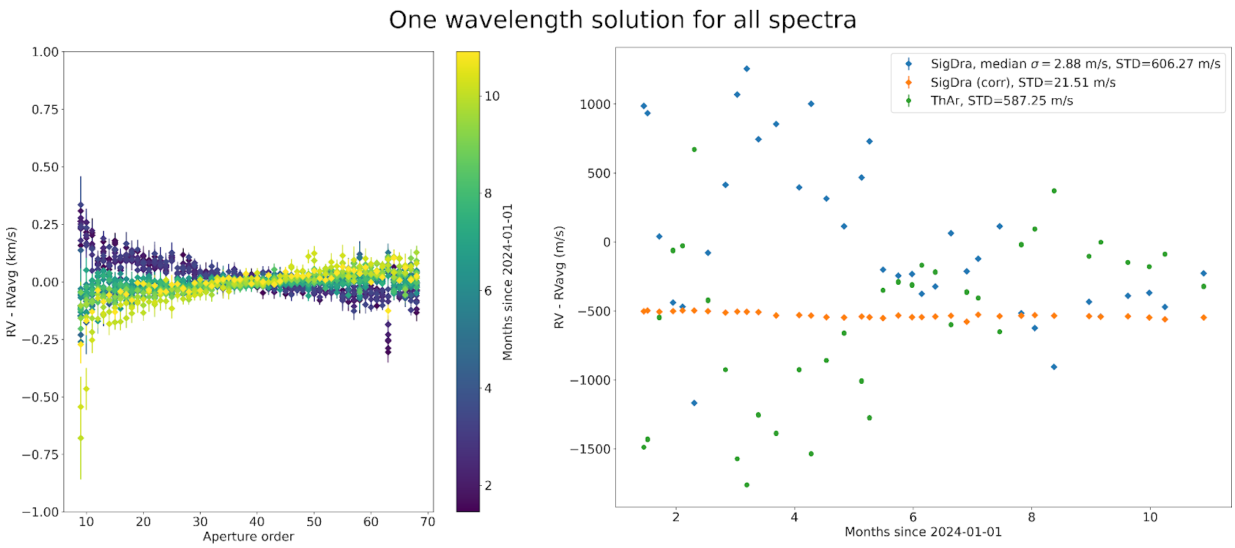

Figure 14. Same as Fig 12 and 13, but for the case where all nights have the same wavelength solution.

In Fig. 14 (left), there are clear, time-variable trends with the order. This is very likely the reason why the ThAr correction applied in Fig. 14 (right) results in a STD of ~22 m/s. The ThAr drift and the stellar RVs are not measured using the same weights across the spectrum, and the wavelength solution does not have high accuracy. As such, unless all time-variable trends in the spectrum can be taken out (e.g. by refitting the wavelength solution), the ThAr spectra become poor correctors. This is further illustrated in the linear regression plots in Fig. 15.

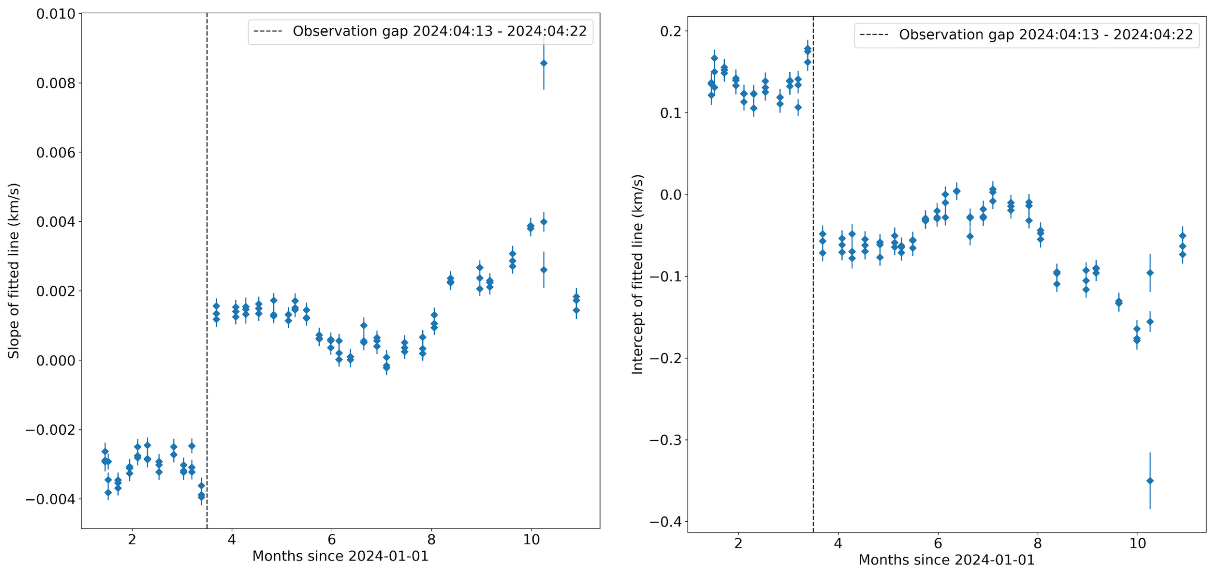

Figure 15. The slope and intercept of a line fit to the orders and RVs of each sig Dra spectrum in Fig. 14 (left).

The large change in April 2024 coincided with the time the spectrograph box was opened in order to adjust the position of the exposure meter pick-off mirror.
Suggestions from staff for possible causes of this change in order-RV behavior has been; changes in the general image like f.ex. rotation of echellogram or focus changes. This effectively limits the feasibility of “fixing” the wavelength solution, unless such effects are characterized, and either stopped or corrected for.

12. Unexplored (potential) systematic sources of uncertainty

For this analysis we have concluded that the wavelength solution is the dominant noise source limiting the error budget. In reality, lack of centering and scrambling can also lead to an uneven distribution of light at the end of the octagonal fiber, and a long-term change in that unevenness might result in a small RV error contribution. We have not explored the impact of the illumination of the science fiber by the ThAr lamp at the fiber exit, and whether or not it changes significantly over the ten month period. This has similarly not been explored for the stellar light either.

To investigate potential time-dependent RV systematics due to changes in the centering of the ThAr lamp, detailed comparisons should be made using independent “RV” sources at different times of year, and different orientations on the sky. This could be done using a combination of standard star observations, the science ThAr lamp, and the calibration fiber ThAr lamp (the lamp in the FIES building). If this is significant, the dome temperature or similar telemetry might correlate with echellogram position.

To explore potential time-dependent RV systematics due to variations in stellar light illumination of the science fiber, multiple standard stars might be needed per night.

13. Action points, software

With this report, it has now been documented that FIES can recover RVs over long periods (10 months in this case), with a stability of 5 m/s, using the standard reduction tools offered through the FIEStool package but an updated linelist of 2200 ThAr lines. The software produced for this analysis was ad-hoc and tailored to the specific project. As such, if a similar data product should to be made available as part of the observatory reduction, a more thorough and robust software must be developed.

FIES is, as expected, not of high enough stability (mechanical, thermal, and barometric) that the wavelength solution can be left fixed for long periods of time, necessitating a frequent refitting using ThAr calibration lamp spectra. The main limiting factor behind the observed 5 m/s limit seems to stem from this refitting procedure. The wavelength solution is significantly more stable close to the lines used for the fit, and can currently reach best-case precision of 1.8 m/s summarizing over all 2200 ThAr lines used. However, this does not reflect the precision further from those lines, and the true accuracy of the wavelength fit in individual pixels is certainly *much* worse than reflected when averaging over all the pixels/lines. Improving the stability of the wavelength fit in areas not as well covered by the linelist will be essential if we wish to ensure long term stability below 5 m/s.

If that is the case, I believe the reduction process should be reconsidered, specifically with the aim of improving stability of the wavelength fit. At the moment, this fitting procedure is used as a catch-all method to re-correct, every night, for both static and dynamic (time-dependent) variations in the observed 2D echellogram, while what should be re-corrected for to ensure stability are only the time-dependent components. For example, since the grating is in a pressurized tank filled with neon, it is likely that the true wavelength dispersion is significantly more stable than the overall image.

The grating equation, which maps order and pixel to wavelength, is approximated using a finite series of orthogonal polynomials, and the larger the strain from systematic sources of uncertainty (optical effects, reduction process, focus), the lower the accuracy of that approximation will be.

We saw an improvement in stability from ~6.5 to 5 m/s by increasing the number of ThAr lines from ~700 to 2200 along with increasing the polynomial degree from 4x4 (16 degrees of freedom (DOF)) to 5x5 (25 DOF). For the time being, it would therefore be beneficial to employ the expanded linelist in the current observatory reduction pipeline for fiber 4.

Increasing the maximum polynomial degree without significant increase in number of ThAr lines will likely not improve stability, and increasing the effective number of useful ThAr lines far beyond 2200 is not feasible with the current reduction methods due to limitations posed by blending and large contrast ratios.

Improvements to the stability of the calibration process could be focused on decreasing the strain on the nightly wavelength solution fit by either; treating each order as independent spectra not connected by the 2D grating equation (as done with the HERMES spectrograph @ MERCATOR); or taking out many of the systematics that can be covered with a static or semi-static theoretical model of the instrument.

We should look to similar non-vacuum spectrographs and inquire their staff for further suggestions on good practices to achieve long-term stability. Examples includes HERMES at the Mercator telescope on la Palma, and SOPHIE at the Observatoire de Haute-Provence in France.

14. Action points, hardware

With the high-resolution fiber 4, the spectral lines are only critically sampled with the current CCD. Additionally, in the corners of the CCD, the spectrograph camera PSF does not produce good image quality, rendering the spectral lines close to the corners of the CCD less suitable for wavelength solution fitting. It would be advantageous for the RV precision to oversample the ThAr arc lines. However, this will come at the cost of reduced SNR per pixel, an effect that could be reduced with a lower noise detector than the current CCD.

Upgrading the camera optics would allow for the use of a larger detector area, and consequently a larger number of spectral features per order for fitting the wavelength solution. Additionally, this would afford the recording of a wider wavelength coverage than what is currently possible, since the CCD crops the spectrum from both the blue and red end.

The main factors limiting the RV short-term precision, with the sandwich method, to the 1-2 m/s level as found in **RD 02**, are still unknown at this moment. Despite the temperature stabilization of the instrument, turbulence is still driven inside the black box and its effects on the RV short-term stability could be studied. The importance of turbulence inside the black box can be measured with a simple Fizeau interferometer setup.

A permanent Fabry-Perot etalon installation should be considered for FIES, since it would offer more lines, better coverage, and better line contrast for wavelength calibration fitting. Better coverage can be achieved with a low-cost commercial off-the-shelf Fabry-Perot filter. However, the affordable Fabry-Perot filters are not intrinsically stable and their drift will need to be monitored with a ThAr arc lamp. Higher stability can be achieved with a vacuum, or noble gas back-filled cavity Fabry-Perot filter. It has been shown by the work of Lars Buchave and René Tronsgaard Rasmussen that a higher stability vacuum cavity can lead to at least a factor of two improvement in long-term stability, from ~5 to ~2-3 m/s, with the current instrumental setup. It should be noted that, during their measurements, the FIES exposure meter was still located inside the black box, affecting the best achievable RV stability.

15. Final words

The interest for high precision and long-term stability in radial velocity measurements on the northern hemisphere (at *and* below 5 m/s) is high for the exoplanet community, as proven by both the current users of FIES, the over-subscription of the HARPS-N at TNG, and current commissioning of the HARPS-3 at INT. While a major hardware upgrade, effectively a full re-design of the spectrograph, would be necessary in order to attempt direct competition with the expensive vacuum instruments purpose-built for planet-finding, reaching a long-term stability similar to the FIES short-term lower limit of ~1 m/s would enable discovery and study of mini-Neptune planets on orbits up to a few years around dwarf stars with mass less than the Sun, or super-Earths on close-in orbits around low-mass M-dwarf stars.

NOT is a telescope built and run on a principle of maximum flexibility in as many fields as possible within the interest of its user base. Most of the current user-countries have dedicated exoplanet groups, and many of those groups use FIES for parts of their observational basis. However, they also spend significant amounts of observing time with very contested spectrographs for observations requiring higher RV precision than FIES can currently offer. Increasing the functionality of FIES, and therefore the NOT, to allow operation deeper within one of the hottest current topics of astrophysics, will help ensure the future support, use and popularity of the telescope, both within the current user basis and outside of it. If this can be achieved without a major hardware upgrade, by updating the instrument software and calibration procedures, and perhaps through relatively minor purchases, it will be a most exceptional bargain.